Electromagnetic form factors of ^{3}H and ^{3}He systems

G J Rampho[1], S A Sofianos[1], S Oryu[2] and T Watanabe[2]

[1] Department of Physics, University of South Africa, Pretoria 0003, South Africa
[2] Department of Physics, Tokyo University of Science, Noda, Chiba 278-8510, Japan

E-mail: rampho@science.unisa.ac.za

Abstract. The angular-momentum-projected and parity-projected Antisymmetrized Molecular Dynamics (AMD) is used to analyze the charge and magnetic form factors of ^{3}H and ^{3}He systems. Non-relativistic nuclear charge and current operators with some relativistic corrections are employed. The Hamiltonian for the nuclear systems is constructed using a realistic nucleon-nucleon potential. The results obtained are in fairly good agreement with the experimental data and therefore the AMD method is a very promising method for use in calculations for electromagnetic form factors of a general A-body nuclear system.

1. Introduction

Charge and magnetic form factors are often used to test model wave functions for the quantum A-body nuclear systems. In such tests one faces the question of a simultaneous accurate description of the form factors and the static properties of the systems. This, of course, presupposes that the model used is able to generate accurately enough, the bound and scattering wave functions needed. In few-nucleon systems this can be achieved using microscopic methods, as for example, those using the Faddeev-type formalisms or methods based on Hyperspherical Harmonics expansion, to extract wave functions for realistic Hamiltonians [1]. These methods are considered, to all practical purposes, to be exact.

This work focuses on the use of a microscopic semi-quantum mechanical method, namely, the AMD method, to study the electromagnetic form factors for the ^{3}H and ^{3}He systems. The AMD approach [2] was developed from the Time-Dependent Cluster Model [3] used in studies of fermionic systems. This approach combines Fermi-Dirac statistics with quantum mechanical assumptions to treat the motion of particles in an A-body system [4] and was previously used to study the dynamics of heavy-ion collisions [5]. It was also used to explain clustering in nuclei as well as angular distributions of scattered protons in proton-nucleus scattering [6]. Furthermore, improved AMD wave functions were constructed that give good predictions in few-body systems [7, 8]. In this work the parity projected and angular momentum projected AMD version [9] is employed to extract the wave functions needed in the calculations.

In Sect. 2 the general formalism of the AMD approach is summarized and the construction of the wave function, the equations of motion of the variable parameters, and the variational technique used are briefly outlined. Results and illustrations of the application of AMD to three-nucleon systems are presented in Sect. 3 while Sect. 4 is devoted to the charge and magnetic form factors, respectively, which are to extract information about ground-state charge and magnetization distributions in the nuclei. Conclusions are drawn in Sect. 5.

2. The AMD formalism

The AMD wave function describing a nuclear system of A nucleons is constructed as a Slater determinant

$$\Psi_{AMD}(\vec{\mathrm{S}}) \;=\; \frac{1}{\sqrt{A!}}\det[\,\phi_j(\alpha,\vec{s}_i),\chi_j(\vec{\sigma}_i),\xi_j(\vec{\tau}_i)\,] \tag{1}$$

where ϕ, χ and ξ are, respectively, the spatial, spin and isospin components of the single-particle wave functions. The spatial components are given in Ref. [5] as Gaussians. The $\vec{s}_i$ are complex variational parameters, $\vec{\mathrm{S}} \equiv \{\vec{s}_1,\vec{s}_2,\vec{s}_3,\ldots,\vec{s}_A\}$ while α is a real constant width parameters The width parameter is a free parameter and taken as common for all the Gaussian functions. The spin-isospin components are fixed in nucleon spin-up or spin-down. A wave function with definite parity(π) and total angular momentum (J) with the angular momentum projection (M) is constructed from the AMD wave function as

$$\Psi^{J\pi}_{MK}(\vec{\mathrm{S}}) \;=\; \frac{1}{2}\,P^{J}_{MK}(\Omega)\,[\,1\pm P^{\pi}\,]\,\Psi_{AMD}(\vec{\mathrm{S}}) \tag{2}$$

where P^{π} is the parity projection operator and $P^{J}_{MK}(\Omega)$ the angular momentum projection operator defined by [10]

$$P^{J}_{MK}(\Omega) \;=\; \frac{2\,J+1}{8\,\pi^2}\int \mathrm{d}\Omega\, D^{J*}_{MK}(\Omega)\,\hat{R}(\Omega). \tag{3}$$

Here $D^{J}_{MK}(\Omega)$ represents the Wigner D-function, $\hat{R}(\Omega)$ the rotation operator and $\Omega \equiv \{\alpha,\beta,\gamma\}$ the Euler rotation angles.

The time-dependent variational principle [5]

$$\delta\int_{t_1}^{t_2}\frac{\langle\,\Psi(\vec{S})\,|\,\mathrm{i}\hbar\,\frac{\partial}{\partial t}-H\,|\,\Psi(\vec{S})\,\rangle}{\langle\,\Psi(\vec{S})\,|\,\Psi(\vec{S})\,\rangle}\,\mathrm{d}t=0 \tag{4}$$

with constraints

$$\delta\Psi(t_1)=\delta\Psi(t_2)=\delta\Psi^{*}(t_1)=\delta\Psi^{*}(t_2)=0\;\;. \tag{5}$$

is used to determine the dynamical equations for the variational parameters. The resulting equations can be transformed to the form [11]

$$\frac{\mathrm{d}\vec{s}_i}{\mathrm{d}t}=-\mu\,\frac{\partial E^{J\pm}_0(\vec{S},\vec{S}^{*})}{\partial\vec{s}^{*}_i}\qquad,\qquad\frac{\mathrm{d}\vec{s}^{*}_i}{\mathrm{d}t}=-\mu\,\frac{\partial E^{J\pm}_0(\vec{S},\vec{S}^{*})}{\partial\vec{s}_i} \tag{6}$$

where μ is an arbitrary positive real constant and

$$E^{J\pm}_0(\vec{S},\vec{S}^{*}) \;=\; \frac{\langle\,\Psi^{J\pm}_{MK}(\vec{\mathrm{S}})|\,H\,|\Psi^{J\pm}_{MK}(\vec{\mathrm{S}})\,\rangle}{\langle\,\Psi^{J\pm}_{MK}(\vec{\mathrm{S}})|\Psi^{J\pm}_{MK}(\vec{\mathrm{S}})\,\rangle}\;\;. \tag{7}$$

the variational energy of the nucleus. Solving these equations minimizes $E^{J\pi}_0$ and determines the variational parameters. The Hamiltonian of the system is given by

$$H \;=\; -\sum_i\frac{\hbar^2}{2\,m_i}\,\nabla^2_i+\frac{1}{2}\sum_{i\neq j}\Big[\,V_{NN}(\vec{r}_{ij})+V_C(\vec{r}_{ij})\,\Big] \tag{8}$$

where m_i is the mass of nucleon i, V_{NN} the two-body nuclear potential and V_C the Coulomb potential. In this work the AV4' NN potential with the $V_{C1}(r)$ Coulomb component is used [12]. The evaluation of the components of the energy expectation values is explained in Ref. [13].

3. Charge form factor

In elastic electron-nucleus scattering, the charge distribution in the nucleus is inferred from the induced electric transitions in the nucleus. The charge form factor is the expectation value of the nuclear charge operator. For a nucleus in an initial state $\mid \Psi^{J_i\pi_i} \rangle$ the charge form factor is given by

$$F_{\rm ch}(\vec{q}) = \frac{1}{Z} \frac{\langle \Psi^{J_i\pi_i} \mid \rho(\vec{q}) \mid \Psi^{J_i\pi_i} \rangle}{\langle \Psi^{J_i\pi_i} \mid \Psi^{J_i\pi_i} \rangle} \tag{9}$$

where Ze is the total charge on and $\rho(\vec{q})$ the charge operator of the nucleus with $\vec{q}$ being the momentum transferred to the nucleus by the electron.

In the plane wave impulse approximation (PWIA) the nuclear charge operator is formed by the superposition of the individual nucleon charge operators and is given by [13]

$$\rho(\vec{q}) = \sum_{k=1}^{A} \left[\frac{q}{Q} G_{Ek}^N(Q^2) - \frac{2\, G_{Mk}^N(Q^2) - G_{Ek}^N(Q^2)}{4\, m_N^2 \sqrt{1+\tau}}\, {\rm i}\vec{\sigma}_k \cdot \vec{q} \times \vec{p}_k \right] \exp(\, {\rm i}\, \vec{q} \cdot \vec{r}_k\,) \tag{10}$$

where $\tau = Q^2/4\, M_N^2$, $Q^2 = q^2 - \omega^2$, $\omega = \sqrt{q^2 + m_N^2} - m_N$ and G_E^N (G_M^N) the nucleon Sachs electric (magnetic) form factor. For the Sachs form factors the phenomenological parameterization derived in Ref. [14] is adopted. The transitions are between states of definite angular momentum. The general multipole analysis of nuclear charge form factors is given by [15]

$$F_{\rm ch}(\vec{q}) = \sqrt{4\,\pi} \sum_{L=0}^{\leq 2J} \langle JJL0|JJ\rangle\, F_L^{\rho}(q)\, Y_{L0}^*(\hat{\mathbf{q}}) \tag{11}$$

where $Y_{LM}^*(\hat{\mathbf{q}})$ are the spherical harmonics, L the nuclear orbital angular momentum and $\langle JJL0|JJ\rangle$ the Clebsch-Gordan coefficients. The summation is over even values of L only. For three-nucleon systems $J_i = \frac{1}{2}$. The intrinsic charge form factor is obtained by dividing the calculated charge form factor by the contributions of the center-of-mass [13].

Using the above definitions, the ground-state charge form factors of the ^{3}H and ^{3}He nuclei are calculated within the PWIA approximation. In this approximation the nucleons inside the target nucleus are assumed non-interacting with one another during the interaction with the electron [17]. This means that the electron interacts with independent nucleons inside the nucleus. The results obtained are displayed in Fig. 1 and Fig. 2. It is noted that the charge form factors are normalized such that $F_{\rm ch}(0) = 1$. As can be seen in these figures, for low momentum transfers, up to the first diffraction minimum, the AMD gives a good description, albeit it slightly overestimates the experimental data. Beyond the first diffraction minimum the results are lower than the data. The first diffraction minimum for the ^{3}H and ^{3}He nuclei are consistent with the predictions of other theoretical models obtained with various nucleon-nucleon potentials [18]. It should be noted that the overestimation of the position of the diffraction minimum indicates an underestimation of the nuclear charge radius.

4. Magnetic form factors

Magnetization density distribution in nuclei are determined from magnetic transitions involving transverse nuclear currents. In the final state of the nucleus is denoted by $|\Psi_{M_f K_f}^{J_f\pi_f}\rangle$, with normalization $\mathcal{N}_{M_f K_f}^{J_f\pi_f}$, the nuclear magnetic form factor is calculated as

$$F_{\rm mag}(\vec{q}) = \frac{1}{\mu_A} \frac{\langle \Psi_{M_f K_f}^{J_f\pi_f} \mid \vec{\mu}(\vec{q}) \mid \Psi_{M_i K_i}^{J_i\pi_i} \rangle}{\sqrt{\mathcal{N}_{M_f K_f}^{J_f\pi_f}\, \mathcal{N}_{M_i K_i}^{J_i\pi_i}}} \tag{12}$$

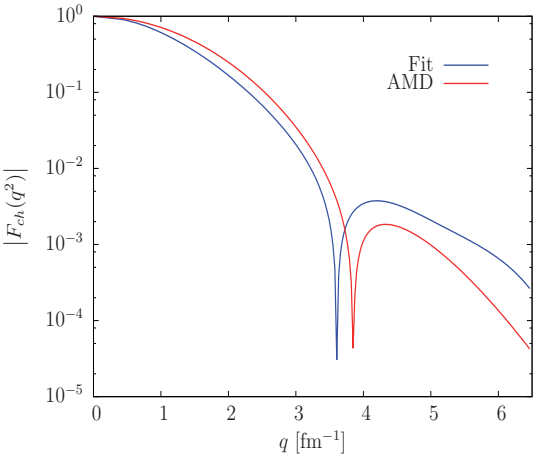

Figure 1. The AMD charge form factor of the ^{3}H nucleus compared with the best fit of the experimental data [16].

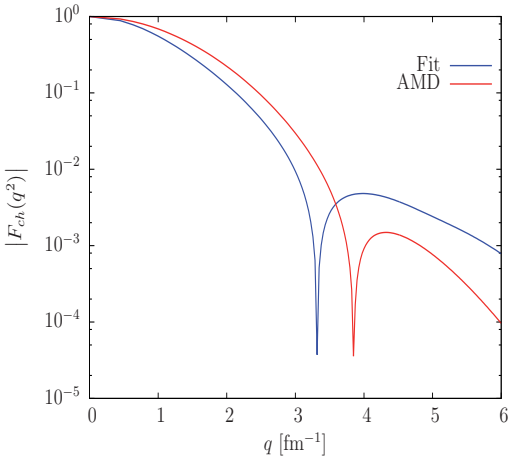

Figure 2. The AMD charge form factor of the ^{3}He nucleus compared with the best fit of the experimental data [16].

where $\vec{\mu}(\vec{q})$ is the magnetization density operator and μ_A the nuclear magnetic dipole moment. The PWIA transverse nuclear magnetization density operator is given by [19]

$$\vec{\mu}(\vec{q}) = \frac{Q}{2\,m_p\,q}\sum_{k=1}^{A}\Big[\,G^N_{Ek}(Q^2)\,\vec{\ell}_k - \mathrm{i}\,G^N_{Mk}(Q^2)\,\vec{q}\times\vec{\sigma}\,\Big]\exp(\,\mathrm{i}\,\vec{q}\cdot\vec{r}_k\,) \tag{13}$$

where $\vec{\ell}_N$ is the nucleon orbital angular momentum. The multipole expansion of nuclear magnetic form factor has the form [15]

$$F_{\rm mag}(\vec{q}) = \frac{\sqrt{4\,\pi}}{\langle JJ10|JJ\rangle}\sum_{L=0}^{\leq 2J}\langle JJL0|JJ\rangle\Big[\,F^{\mu}_{LL-1}(q)\,\mathbf{Y}^{0*}_{LL-1}(\hat{\mathbf{q}}) + F^{\mu}_{LL+1}(q)\,\mathbf{Y}^{0*}_{LL+1}(\hat{\mathbf{q}})\,\Big] \tag{14}$$

where the summation is over odd values of L,

$$\mathbf{Y}^{0*}_{LM}(\hat{\mathbf{q}}) = \sum_m \langle Mm1\,{-m}|L0\rangle\,Y_{Mm}(\hat{\mathbf{q}})\,\hat{\mathbf{e}}_m\,. \tag{15}$$

are the vector spherical harmonics and $\hat{\mathbf{e}}_m$ spherical unit vectors.

The general form of the nuclear magnetic transition multipole operator can be derived as in Ref. [20] for a given nuclear current operator. The intrinsic magnetic form factor of the systems is obtained by factoring out the contributions of the center-of-mass from Eq. (14). The results obtained for the magnetic form factors for three-nucleon systems are displayed in Fig. 3 and Fig. 4 and compared with the best fit to the experimental data [16]. Similarly to the charge form factors, the magnetic form factors are normalized such that $F_{\rm mag}(0) = 1$. As can be seen, the AMD form factors reproduce the experimental data reasonably well at low momentum transfer, for both systems. The position of the first diffraction minimum is underestimated. However, at momentum transfer greater than the diffraction minimum the AMD results are unsatisfactory and are not consistent with theoretical results obtained with other approaches [21].

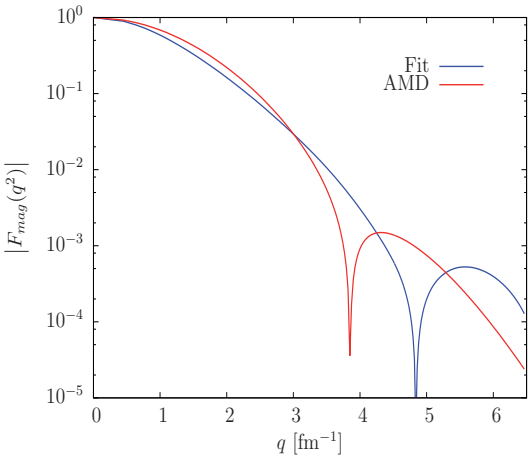

Figure 3. The AMD magnetic form factor of the ^{3}H nucleus compared with the best fit of the experimental data [16].

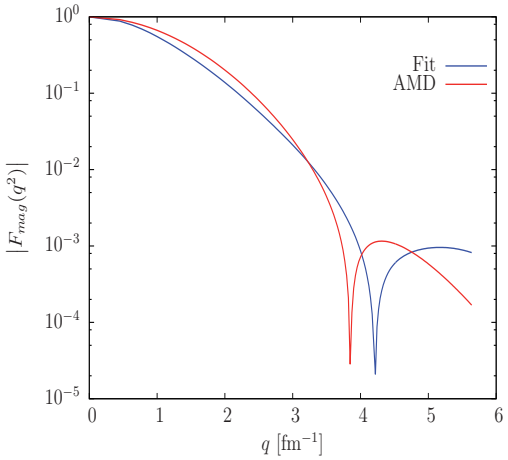

Figure 4. The AMD magnetic form factor of the ^{3}He nucleus compared with the best fit of the experimental data [16].

5. Conclusions

We employ the angular-momentum-projected and parity-projected antisymmetrized molecular dynamics to calculate the charge and magnetic form factors for the ^{3}H and ^{3}He systems. The charge monopole and the magnetic dipole transitions in the nuclei were determined from elastic electron scattering. In overall, the results obtained, within the AMD and PWIA approximation, reproduce the general behavior of the experimental form factors. For both, the charge and magnetic form factors, and for momentum transfer below the first diffraction minimum the reproduction is fairly good. However, beyond the first diffraction minimum the results for the charge form factor are lower than the data while the results for the the magnetic form factor are less satisfactory. The deviations of the theoretical results from experimental data can be minimize once better wave functions can be employed. These can be constructed by using a more complete realistic Hamiltonian, three-body forces, and relativistic corrections in the electromagnetic operators used. It should be noted that these results are consistent with other results obtained by competing theoretical models.

In conclusion, the results indicate that the AMD method is a very promising method in calculating electromagnetic form factors of the general A-body nuclear system.

Acknowledgments

This work is part of a PhD thesis submitted to the University of South Africa.

References

[1] Kamada H *et al*, 2001 *Phys. Rev.* C**64** 044001
[2] Horiuchi H, 1991 *Nucl. Phys.* **A 522** 257c
[3] Caurier E, Grammaticos B, and Sami T, 1982 *Phys. Lett.* **B 109** 150
[4] Feldmeier H, 1990 *Nucl. Phys.* **A 515** 147
[5] Ono A, Horiuchi H, Maruyama T and Ohnishi A, 1992 *Prog. Theor. Phys.* **87** 1185
[6] Tanaka E I, Ono A, Horiuchi H, Maruyama T, and Engel A, 1995 *Phys. Rev.* C **52** 316
[7] Togashi T, Kat$\bar{o}$ K 2007 *Prog. Theor. Phys.* **117** 189
[8] Watanabe T and Oryu S, 2006 *Prog. Theor. Phys.* **116** 429
[9] Kanada-En'yo Y, Horiuchi H, and Ono A, 1995 *Phys. Rev.* C**52** 628
[10] Peierls R E and Yoccoz J, 1957 *Proc. Phys. Soc.* **A 70** 381
[11] Ono A and Horiuchi H, 2004 *Prog. Part. Nucl. Phys.* **53** 501
[12] Wiringa R B and Pieper S C, 2002 *Phys. Rev. Lett.* **89** 182501-1

[13] Rampho G J, 2010 *PhD Thesis*, University of South Africa, unpublished.
[14] Friedrich J and Walcher Th, 2003 *Eur. Phys. J.* **A 17** 607
[15] Überall H, 1971 *Electron Scattering from Complex Nuclei*, Part A (Academic Press, New York)
[16] Amroun A, Breton V, Cavedon J -M, Frois B, Goutte D, F. P. Juster F P, Leconte Ph, Martino J, Mizuno Y, Phan X -H, Platchkov S K, Sick I, Williamson S, 1994 *Nucl. Phys.* **A 579**, 596
[17] Chew G F and Wick G C, 1952 *Phys. Rev.* **85** 636
[18] Kloet W M and Tjon J A, 1974 *Phys. Lett.* **B 49** 419
[19] Ciofi degli Atti C, 1980 *Prog. Part. Nucl. Phys.* **3** 163
[20] Willey R S, 1963 *Nucl. Phys.* **40** 529
[21] Hadjimichael E, Goulard B, and Bornais R, 1983 *Phys. Rev.* C**27** 831